NANO LETTERS

Letter

pubs.acs.org/NanoLett

A Half Millimeter Thick Coplanar Flexible Battery with Wireless Recharging Capability

Joo-Seong Kim,[†,‡] Dongah Ko,[†] Dong-Joo Yoo,[†,‡] Dae Soo Jung,[§] Cafer T. Yavuz,[†] Nam-In Kim,[∥] In-Suk Choi,[⊥] Jae Yong Song,*[,#] and Jang Wook Choi*[,†,‡]

[†]Graduate School of Energy, Environment Water, and Sustainability (EEWS) and [‡]Center for Nature-inspired Technology (CNiT) in KAIST Institute NanoCentury, Korea Advanced Institute of Science and Technology (KAIST), 291 Daehak-ro, Yuseong-gu, Daejeon 305-338, Republic of Korea

[§]Eco-Composite Materials Team, Korea Institute of Ceramic Engineering & Technology (KICET), 77, Digital-ro 10-gil, Guemcheon-gu, Seoul 153-801, Republic of Korea

[∥]R&D Center, Rocket Electric, 147-46 Yangil-ro, Buk-gu, Gwangju 500-866, Republic of Korea

[⊥]High Temperature Energy Materials Research Center, Korea Institute of Science and Technology (KIST), 5, Hwarang-ro 14-gil, Seongbuk-gu, Seoul 136-791, Republic of Korea

[#]Center for Nanomaterials Characterization, Korea Research Institute of Standards and Science (KRISS), 267 Gajeong-ro, Yuseong-gu, Daejeon 305-340, Republic of Korea

S *Supporting Information*

ABSTRACT: Most of the existing flexible lithium ion batteries (LIBs) adopt the conventional cofacial cell configuration where anode, separator, and cathode are sequentially stacked and so have difficulty in the integration with emerging thin LIB applications, such as smart cards and medical patches. In order to overcome this shortcoming, herein, we report a coplanar cell structure in which anodes and cathodes are interdigitatedly positioned on the same plane. The coplanar electrode design brings advantages of enhanced bending tolerance and capability of increasing the cell voltage by in series-connection of multiple single-cells in addition to its suitability for the thickness reduction. On the basis of these structural benefits, we develop a coplanar flexible LIB that delivers 7.4 V with an entire cell thickness below 0.5 mm while preserving stable electrochemical performance throughout 5000 (un)bending cycles (bending radius = 5 mm). Also, even the pouch case serves as barriers between anodes and cathodes to prevent Li dendrite growth and short-circuit formation while saving the thickness. Furthermore, for convenient practical use wireless charging via inductive electromagnetic energy transfer and solar cell integration is demonstrated.

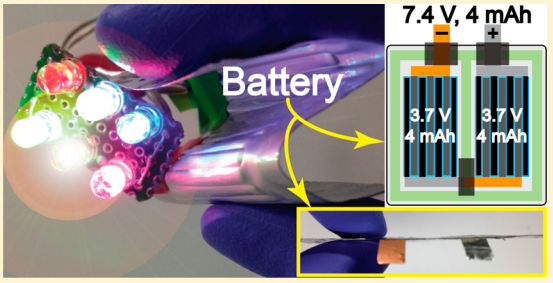

KEYWORDS: *Coplanar structure, flexible battery, interelectrode barrier, lithium ion battery, wireless charging*

IT technology is currently entering a new era represented by flexible and wearable electronics. Toward this new paradigm, a vast number of concepts and functions have already been demonstrated[1−4] on plastic, paper, and textile substrates that replace conventional flat and rigid counterparts made of semiconductor and glass. Along the direction, sensors,[5−7] light-emitting diodes (LEDs),[8−10] energy-harvesting devices,[11−14] and other circuit elements[15−18] have been conceptualized and realized as key components on those flexible substrates. Besides these components, for development of a fully functional flexible/wearable platform a power source should also be integrated together to ensure the portable capability of the entire platform.

The battery community has recognized this rising demand for a while and has invested considerable efforts to develop flexible/wearable lithium rechargeable batteries.[19−31] One of the main research directions was to develop current collectors with tolerance against folding/bending motions and combine them with existing redox-active battery materials.[22−28,30] To this end, conductive carbon nanomaterials, such as graphene and carbon nanotubes, were fabricated as free-standing films or coated onto paper and textiles. In the latter configurations, in particular both nanometer dimensions of the carbon materials and 3D porous structures of paper and textiles play a synergistic role in achieving robust electrochemical operations under bending/folding motions by releasing the bending-induced stress and maintaining the adhesion of active components onto the current collectors. Similarly, the structural advantage of paper and textiles were combined with electroless deposition to coat textiles with highly conductive metals.[22,23,32] The carbon

Received: November 29, 2014
Revised: February 26, 2015
Published: March 2, 2015

DOI: 10.1021/nl5045814
Nano Lett. 2015, 15, 2350−2357

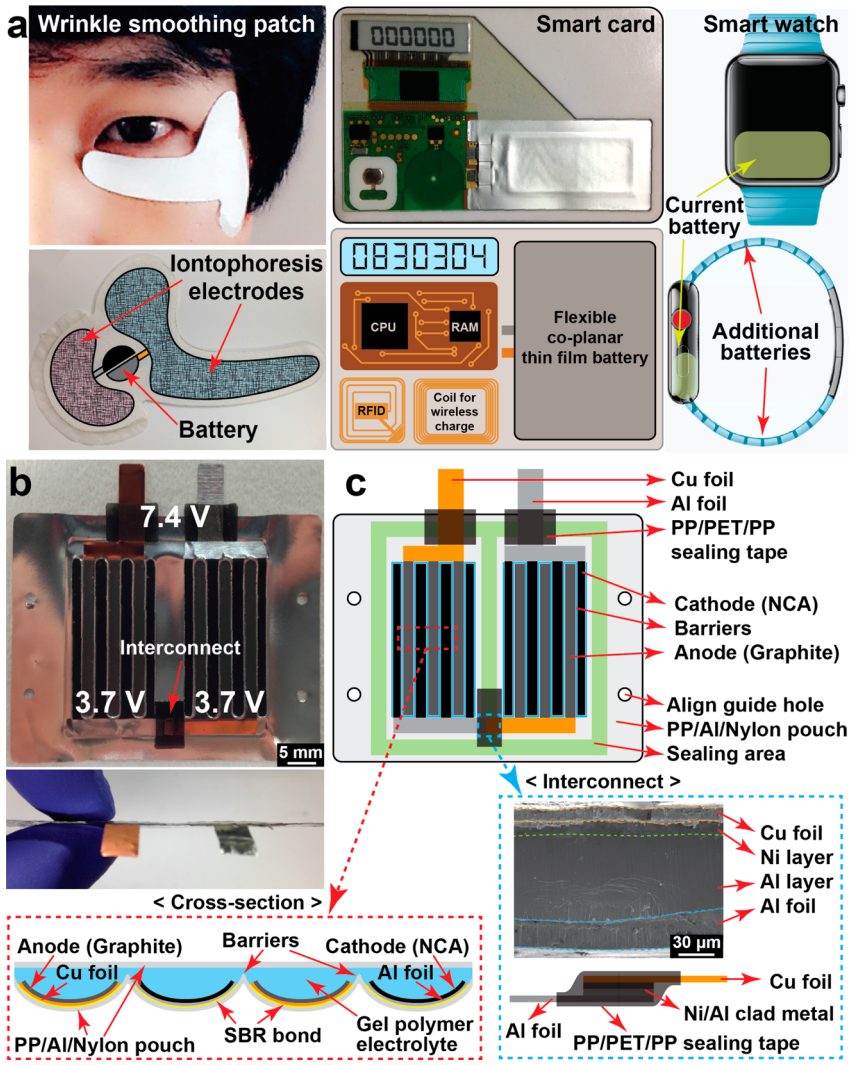

Figure 1. (a) Potential applications of coplanar flexible batteries. (Left) A medical/cosmetic patch with iontophoresis function, (middle) a smart card with other accessory components installed, and (right) a smart watch with a supplementary battery in the watchstrap. (b) Top-viewed and cross-sectional photographs of a coplanar flexible battery in which two of 3.7 V cells are connected in series. (c) Schematic illustration of a coplanar flexible battery showing the cell configuration composed of interdigitated electrodes, interconnect, metal tails for external electric connection, and pouch. (Bottom left) A cross-sectional illustration of the interdigitated electrodes with pouch barriers between adjacent anodes and cathodes by the curvy geometry of each electrode. (Bottom right) Ni/Al clad metal intermediate layers to bridge Al and Cu interconnects. Al and Cu are not feasible to be directly welded.

nanomaterials in the same electrode platforms were also used as active materials to demonstrate flexible/wearable supercapacitors.[33−40] See Table S1 in Supporting Information for detailed properties of recent flexible lithium rechargeable batteries.

While these research outcomes have served as a solid basis in ripening flexible/wearable lithium ion battery (LIB) technology, their physical dimensions should be considered carefully depending on the target applications. In fact, many potential applications of flexible/wearable LIBs, such as smart cards and medical/cosmetic patches, are very sensitive to the thickness. If the final thicknesses are increased too much after the integration of additional batteries and circuit components, the whole assembled items could lose comfort and may not be adopted from users. Previously, stable operations of flexible thin film LIBs were demonstrated by sequentially depositing active ceramic layers via a sputtering process.[41,42] Nevertheless, it may be preferred to develop new cell configurations beyond the cofacial structure where anode, separator (or electrolyte), and cathode are stacked in consecutive layers because such structure has a limitation in lowering the cell thickness due to its intrinsic stacking geometry. Moreover, the cofacial structure is not intrinsically supportive of bending motions because each layer would undergo different tensile/compressive stress during the bending motions and generate friction force against the neighboring layers, leading to peeling off of the active components from the electrodes (Supporting Information Figure S1).

To overcome these inherent shortcomings of the cofacial structure, in the present investigation we have introduced a flexible thin LIB based on a coplanar structure where anode and cathode are interdigitatedly positioned in the same plane of a limited thickness. The key design in this coplanar structure is to take aluminum pouch as an active cell component and use it as barriers between the anodes and cathodes because these barriers can prevent fatal short-circuits routinely occurring between the neighboring electrodes during bending motions while saving the thickness. On the basis of this structural benefit, the final cell thickness is only 0.5 mm, which is even

DOI: 10.1021/nl5045814
Nano Lett. 2015, 15, 2350−2357

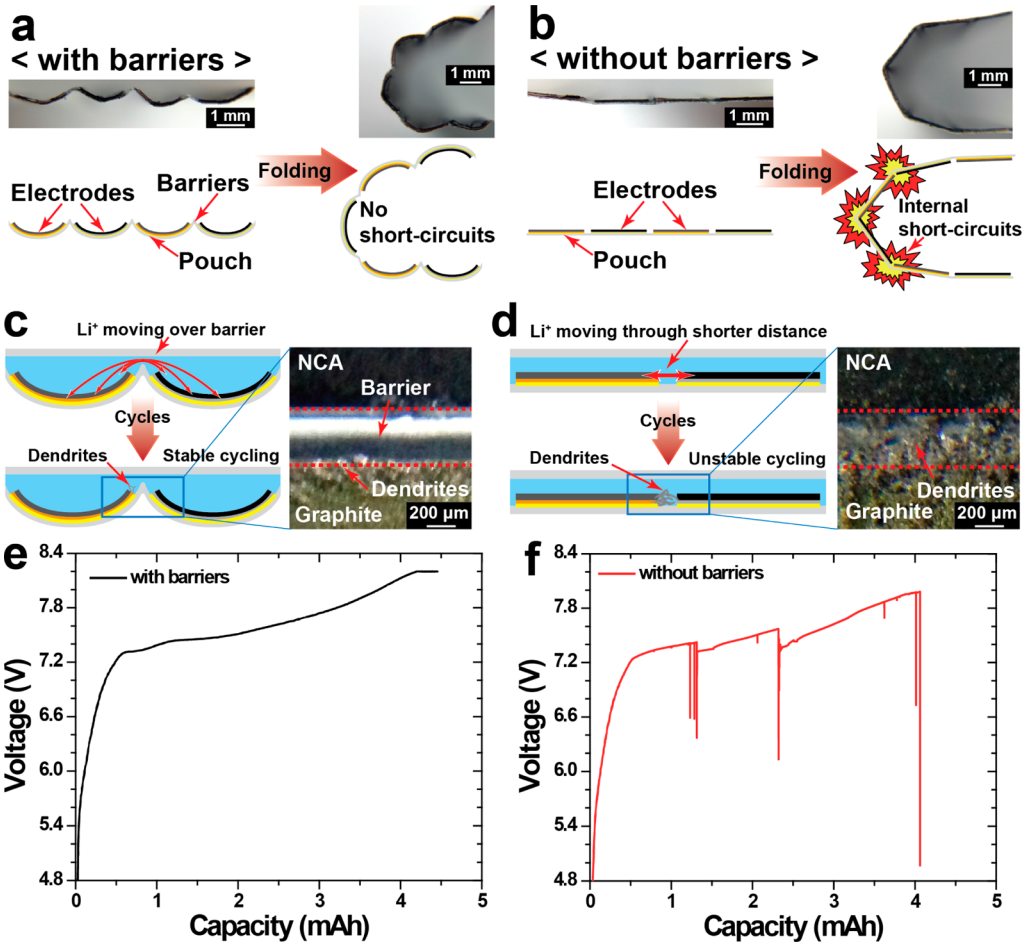

Figure 2. (a) The digital photograph and schematic view of the coplanar LIB with barriers and curvy electrode shape, revealing the importance of both structural features in preventing short-circuits between neighboring anodes and cathodes. (b) The same coplanar electrodes without barriers and curvy structure suffering from short-circuits between adjacent electrodes upon folding. (c,d) The effect of barriers in suppressing overgrowth of Li dendrites during repeated cycles. The graphical illustration showing distinct Li diffusion pathways that affect Li dendrite growth, along with top-viewed microscopic images taken at the end of the first charge. The first charging profiles of a coplanar battery (e) with and (f) without barriers. The cell without barriers shows incomplete charging and sudden voltage drops due to short-circuits caused by Li dendrite growth.

smaller than those (~0.8 mm) of typical credit cards, while robust electrochemical operations are retained during aggressive (un)bending cycles. Furthermore, the two-dimensional (2D) electrode configuration allows the modification of its pattern for sequential addition of a single-cell voltage, which in our case is to 7.4 V by series connection of two 3.7 V cells. The 2D planar structure also allows us to integrate the battery with wireless charging components based on inductive electromagnetic energy transfer or solar energy on the same plane. The coplanar interdigitated structure has been used only in microbatteries in 100−500 μm scale,[43] and to the best of our survey the current study is the first such demonstration for bulk flexible applications.

The present flexible thin LIBs are targeted for medical/cosmetic patches with iontophoresis functions, smart cards with purposes of personal identification, financial transit, wireless communication, health care, and other information storage as well as watchstraps serving as supplementary power sources (Figure 1a). A photograph of the complete cell before final pouch sealing and a schematic illustration of the corresponding cell configuration are presented in Figure 1b,c, respectively. In the coplanar interdigitated configuration, the width of each anode or cathode is 2 mm except for the outer cathodes (1.5 mm), and the anodes and cathodes are 400 μm apart from each other. The fork-shaped electrodes were patterned by punching copper (Cu) or aluminum (Al) foil with the electrodes pasted on top using knife molds made of steel (Supporting Information Figure S2). While a detailed fabrication flow including barrier formation, electrode attachment, and pouch sealing is presented in Experimental Section and Supporting Information Figure S3, it is noteworthy that the curvy shape of each electrode was achieved simply by processing the punching step on a soft acryl resin substrate (Supporting Information Figure S2). It is also remarkable that ultrasonic welding of a Ni/Al clad metal pad was employed between Cu and Al foils at an interconnecting point for in-series connection of two cells because Cu and Al are known to be very difficult to be welded into a direct contact via a normal ultrasonic welding process.

The interelectrode barriers constituted by a pouch together with curvy electrode structure play a very critical role in robust electrochemical performance, especially during bending motions. First, the barriers and the curvy electrode structure prevent short-circuits between anodes and cathodes. While the barriers physically block the direct contact between both adjacent electrodes, the curvy structure leads to a bending geometry where the whole structure is divided into series of arcs and both ends of each arc remain separate from the neighboring ones (see Figure 2a). By contrast, the control case

DOI: 10.1021/nl5045814
Nano Lett. 2015, 15, 2350−2357

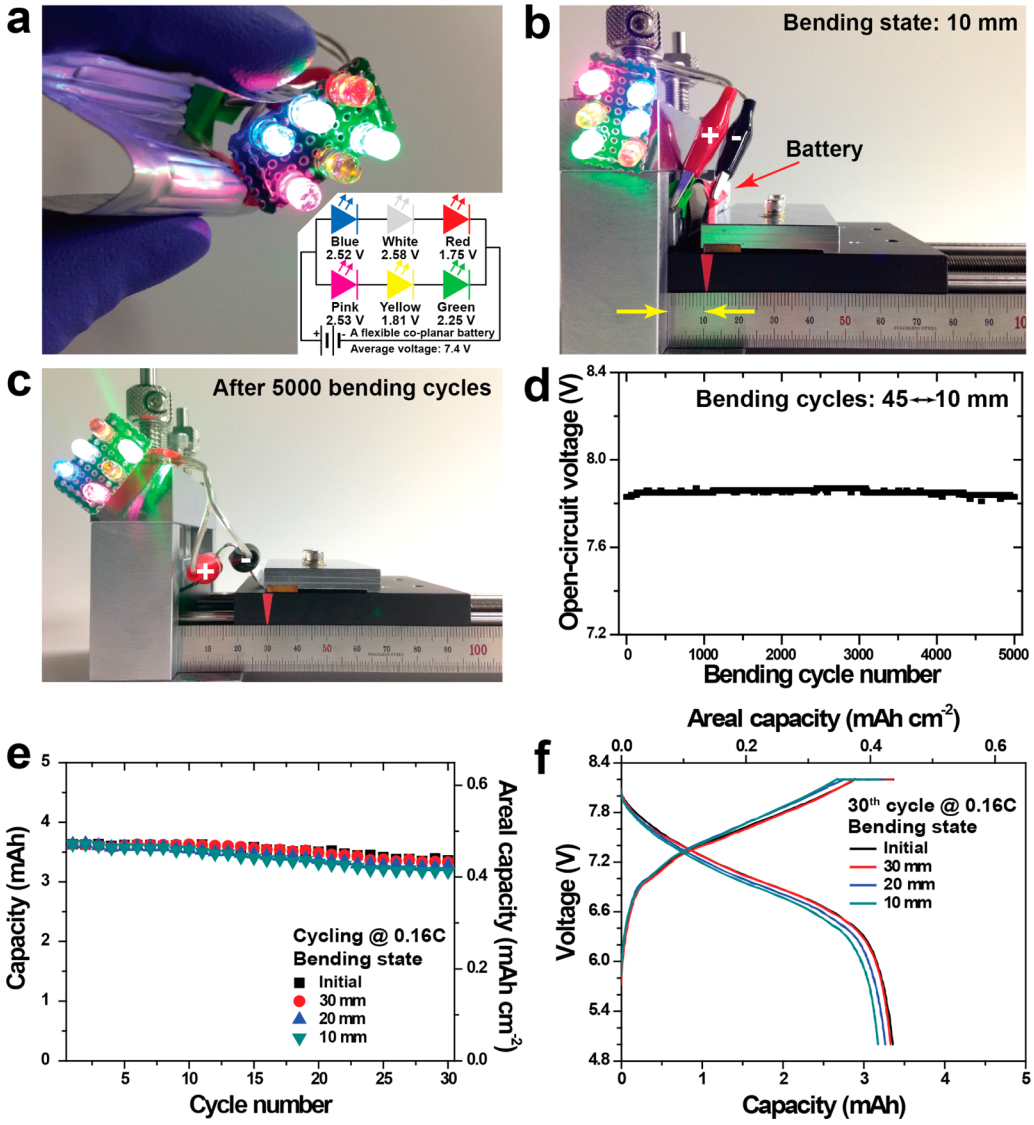

Figure 3. Demonstration of bending capability of the coplanar flexible LIB. (a) Lighting up six LEDs under a bent condition. (Inset) An equivalent circuit showing the connection of six LEDs together with voltage consumption from each LED. The LED tests of the coplanar flexible LIB at bending states of (b) 10 mm after 1 (un)bending cycle and (c) 30 mm after 5000 (un)bending cycles. (d) OCVs under charged state at different cycle numbers. The bending in each cycle is all the way to 10 mm. (e) The discharging capacity retentions under different bending states at 0.16C and 25 °C and (f) their corresponding charge−discharge profiles at the 30th cycles.

without the barriers (Figure 2b) is liable to direct touching between the adjacent electrodes due to rigid bending at each bending hinge, which could result in fatal electrochemical performance. More seriously, the presence of the barriers prevents Li dendrite growth (Figure 2c−f). In the coplanar configuration, metal current collectors are inevitably exposed to incoming Li ions so that Li dendrites can grow on the current collectors while Li ions simultaneously intercalate into active electrode materials. Once the barriers are formed between both electrodes, however, Li ions tend to diffuse dominantly toward the top surfaces of the electrodes (see the red arrows in Figure 2c), and as a result the dendrite growth is suppressed significantly. The barrier effect against Li dendrite growth was indeed verified in the optical microscope images of both cases as shown in insets of Figure 2c,d taken after the first charge without bending motions. The same effect was also reflected in the electrochemical profiles. While the sample with the barriers exhibited a clean first charging profile (Figure 2e), the control sample without the barriers showed sudden voltage drops in the middle of the charge (Figure 2f). More critically, the profile was not able to reach the top cutoff voltage of 8.2 V even in the first charge again due to short-circuit formation originating from severe Li dendrite growth.

The bendability and robust electrochemical performance of the coplanar thin battery was first verified by testing with light-emitting diodes (LEDs) (Figure 3a). Six LEDs with different colors were connected in series and parallel as shown in inset of Figure 3a with the voltage consumption of each LED denoted. Our cell voltage of 7.4 V is large enough to cover the overall voltage drops (~6.85 V) by LEDs. The operation of the LEDs was examined at different bending states, defined as end-to-end distance along the bending direction, from 45 to 10 mm (see the rulers in Figure 3b,c, and Supporting Information Figure S4). At all of these bending states, all of the LEDs remained operational with persistent voltage supply (see Supporting Information Movie S1 and S2), supporting its excellent bending

DOI: 10.1021/nl5045814
Nano Lett. 2015, 15, 2350−2357

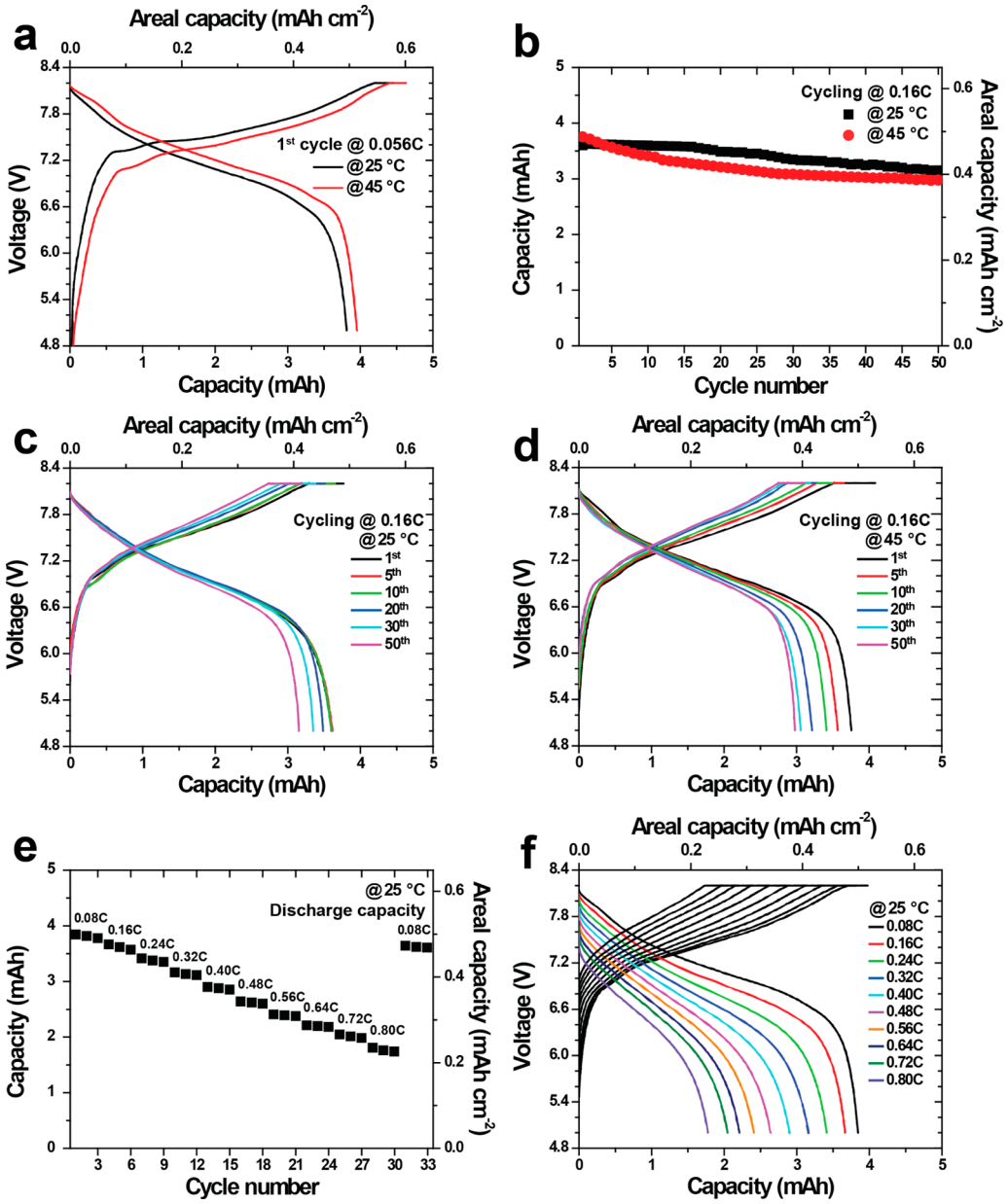

Figure 4. Electrochemical performances of a coplanar flexible LIB. (a) The first charging and discharging voltage profiles at 25 and 45 °C. (b) The discharging capacity retentions at 0.16C at 25 and 45 °C and (c,d) their corresponding voltage profiles. (e) Summarized rate capability at 25 °C and (f) its corresponding voltage profiles at various C-rates (1C = 3.875 mA).

tolerance. Even when (un)bending cycle with a 10 mm end-to-end distance was repeated for 5000 times, the coplanar LIB was still able to light up the LEDs (Figure 3c), reconfirming the robust mechanical endurance. In the same line, when open-circuit voltage under charged state was monitored during repeated (un)bending cycles, its value turned out to be quite stable around 7.8 V over the entire 5000 cycles (Figure 3d). When tested under different bending states imposed throughout cycling, the bending states of 10, 20, and 30 mm and initial state with no bending retained similar discharge capacity retentions of 87.5, 89.9, 91.7, and 92.9%, respectively, after 30 cycles (Figure 3e). Their corresponding charge−discharge profiles at the 30th cycles are displayed in Figure 3f.

The electrochemical performance of the coplanar thin battery was evaluated more quantitatively under the galvanostatic mode (Figure 4). Graphite and $LiNi_{0.8}Co_{0.15}Al_{0.05}O_2$ (NCA) were used as anode and cathode active materials, so the current coplanar LIB in which two 3.7 V cells are connected in series delivers ∼7.4 V as indicated by its first charge−discharge profiles measured at 0.056C (1C = 3.875 mA) at 25 and 45 °C (Figure 4a). Also, once converted to the gravimetric value, the observed capacity of 3.82 mAh becomes 130 mAh g^{-1} with respect to the mass of cathode active material. This coplanar LIB showed robust cycling performance, as it exhibited 87.5 and 79.3% capacity retentions after 50 cycles at 25 and 45 °C, respectively (Figure 4b). The corresponding voltage profiles at different cycling numbers are presented in Figure 4c,d. This coplanar LIB also exhibited decent rate capability in a way that the cell retained 89, 76, and 47% of the original capacity upon C-rate increase from 0.08 to 0.24, 0.40, and 0.80C as displayed in Figure 4e,f. The observed cell performance implies that the interelectrode distance is short

DOI: 10.1021/nl5045814
Nano Lett. 2015, 15, 2350−2357

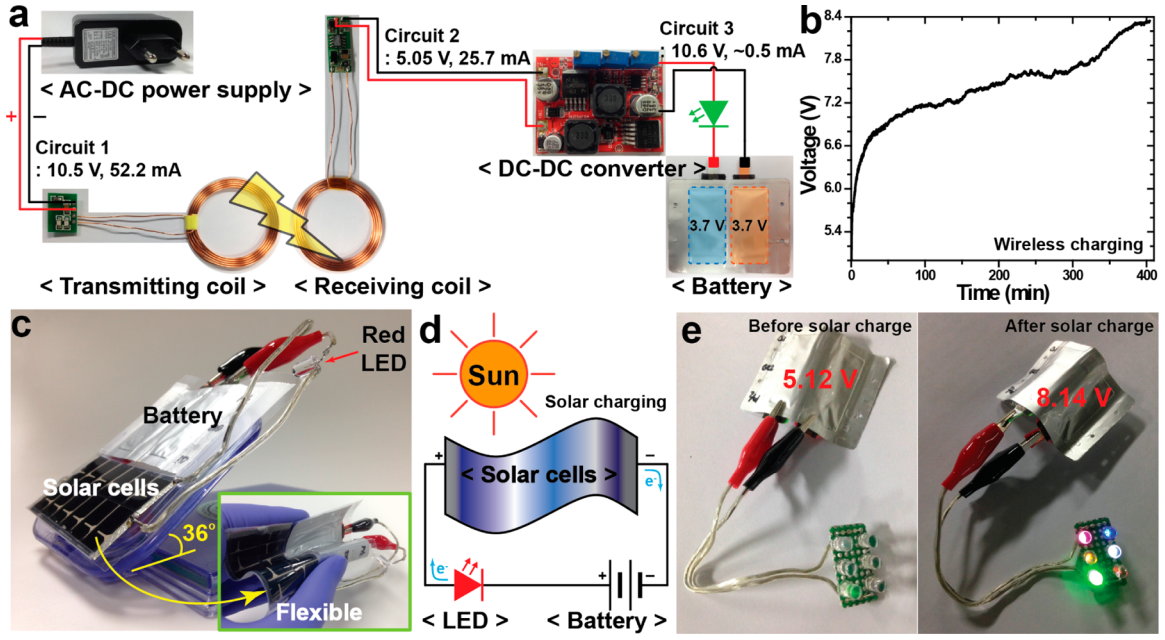

Figure 5. Wireless recharging. (a) A scheme of an energy transfer circuit by electromagnetic induction together with current and voltage information at different circuit points. (b) A voltage profile during the charging based on the inductive electromagnetic energy transfer process. (c) A platform consisting of both the coplanar LIB and a commercial flexible solar cell and (d) its equivalent circuit. (e) The tests with LEDs before and after solar charging alongside the cell voltages at both states.

enough to facilitate good Li ion diffusion between both electrodes within reasonable charge−discharge durations. However, short interelectrode distances could in turn make the cell vulnerable to detrimental short-circuits from Li dendrite growth in the coplanar structure. Thus, the interelectrode pouch barriers play a very crucial role in overcoming the trade-off situation between electrode performance and Li dendrite growth. More advanced cell design to decrease the interelectrode distance and thus improve the rate performance must be feasible by employing more delicate fabrication processes such as printing technique.

For long-term convenient use of these thin flexible LIBs, it is desirable to have wireless recharging capability. To demonstrate such opportunities, an energy transfer circuit by electromagnetic induction and a solar cell were combined with a coplanar LIB (Figure 5). In order to demonstrate the recharging capability based on an energy transfer circuit, a coplanar LIB was sequentially connected to a dc−dc converter and a receiving coil, as displayed in Figure 5a. The receiving coil acquires induced electromagnetic energy from a transmitting coil in a distance around 1 cm, and the subsequent circuit (Circuit 2) produces 5.05 V and 25.7 mA. A dc−dc converter was followed to provide proper voltage and current (Circuit 3, 10.6 V, and ~0.5 mA) for battery charging. On the transmitting coil side, a transmitting coil (Circuit 1, 10.5 V and 52.2 mA) was connected to an ac−dc power supply. Although the receiving coil and the dc−dc converter were separately located in the current demonstration, their monolithic integration onto the same platform as the battery would be feasible by engaging soft electronic fabrication processes[44] and will be introduced in detail in forthcoming publication. Also, once the monolithic integration becomes available, the dimensions of the coils and other accessory circuits can be decreased accordingly by consideration of the target current level for recharging. Wireless charging by the energy transfer circuit was indeed achieved as indicated by its charging curve in Figure 5b. For solar charging capability, a coplanar LIB was connected to a commercially available flexible solar cell. A photograph of the complete solar charging system and its equivalent circuit are shown in Figure 5c,d, respectively. For the solar cell operation, to maximize the power conversion efficiency the angle of the assembled platform was set to 36° from the ground. A red LED was also included in the circuit to ensure the actual charging and also prevent reverse current flow. After 8 h exposure to sunlight during daytime, the cell under the discharged state of 5.12 V was fully charged to 8.14 V (Figure 5e). Detailed solar cell conditions and voltage/current values are provided in Experimental Section.

In conclusion, robust bending capability and stable electrochemical performance of a thin flexible LIB were achieved by a combined approach of the coplanar electrode geometry and interelectrode barriers. While the coplanar interdigitated electrode configuration allows the limitation of the overall cell thickness below 0.5 mm with capability of releasing the stress originating from (un)bending motions, the interelectrode barriers overcome the issues intrinsic to the coplanar geometry including short-circuits and Li dendrite growth. The current coplanar LIBs can be readily integrated onto various physical platforms, such as patches, cards, and watchstraps, and can thereby contribute to expanding the functions of the host platforms. The present interdigitated electrode configuration can also be produced by diverse printing techniques to produce more delicate patterns at higher speed.

Experimental Section. *Coplanar Cell Fabrication.* For the anode fabrication, slurry was first prepared by dispersing graphite (Showa denko, Supporting Information Figure S5a), denka black, and polyvinylidene fluoride (PVDF, Arkema) in a weight ratio of 85.5:4.5:10. The slurry was cast onto Cu foil by the doctor blading method, and the final electrode loading was ~11 mg cm^{-2} after complete drying. The cathode was prepared in the same procedure, but $LiNi_{0.8}Co_{0.15}Al_{0.05}O_2$ (NCA, Ecopro, Supporting Information Figure S5b), denka black, and PVDF

DOI: 10.1021/nl5045814
Nano Lett. 2015, 15, 2350−2357

were used in the slurry formation in a 94:3:3 weight ratio. The slurry was cast onto Al foil, and the final electrode loading was ~14 mg cm^{-2}. The n/p ratio defined by total anode capacity/total cathode capacity was ~1.12, and the total capacity from the 7.4 V cell is 3.82 mAh at 0.056C. Both electrodes were then punched off into a fork-shaped pattern (inner electrode width = 2 mm, outer electrode width = 1.5 mm, Supporting Information Figure S6) using a knife mold (Supporting Information Figures S2 and S6). Meanwhile, the barriers were formed from the bottom pouch by placing a template and pressing it (top picture in Supporting Information Figures S3 and S6e). The SBR bond was spray onto the backsides of the electrodes, and both electrodes were then attached onto the bottom pouch following its barrier pattern. A Ni/Al clad metal pad was used for in-series connection of two cells. The pad was located between Cu and Al foils at the interconnect with the Al side of the pad facing the Al foil. The connection was completed by an ultrasonic welding process. In order to protect this connection from corrosion during the exposure to the electrolyte, sealing tape was attached all around the connection. Next, the top pouch was attached on the center area after being aligned based on aligning holes, and gel electrolyte (25 wt %, polyvinylidene fluoride-*co*-hexafluoropropylene (PVDF-HFP) in ethylene carbonate (EC)/diethylenecarbonate (DEC) = 1:1 = v/v containing 1.15 M lithium hexafluorophosphate ($LiPF_6$) and 5 wt % fluoroethylene carbonate (FEC), Supporting Information Figure S7) was injected from both sides, followed by vacuum sealing of the entire pouch. The area occupied solely by the interdigitated electrodes in each 3.7 V cell is 3.9 cm^2 (Figure 1b and Supporting Information Figure S6).

Electrochemical Testing. The completed coplanar battery in which two of 3.7 V NCA/graphite full-cells that were connected in series was tested at 25 and 45 °C without a battery management system to balance the charging for each battery. The electrochemical measurements were performed in the full-cell voltage range of 5.0−8.2 V using a battery cycler (MACCOR series 4000). For all of the electrochemical measurements, charging and discharging processes were under the constant current and constant voltage (CCCV) and constant current (CC) modes, respectively. In order to measure ionic conductivities of the gel electrolyte at various concentrations, electrochemical impedance spectroscopy (EIS, Bio-Logic VSP) measurements were conducted in the frequency range of $0.01-10^6$ Hz by using symmetric stainless steel for both electrodes with a 400 μm gap.

Wireless/Solar Charging. As illustrated in Figure 5a, for the recharging based on an energy transfer circuit via electromagnetic induction, the coplanar battery was connected to a dc-to-dc converter (LM2577S/LM2596S dc 4−35 V to 1.25−25 V and 0−4 A voltage/current adjustable automatic buck-boost converter) and sequentially to a receiving coil (diameter ~3.8 cm, Seeed Technology). On the transmitting coil side, the same coil was wired to an ac−dc power supply (switched-mode power supply (SMPS), 12 V) for hooking-up to a power outlet. For the solar charging, we used a commercial flexible solar cell (power conversion efficiency: ~3.8%, PowerFilm Solar). For voltage matching with the coplanar LIB, 12 unit cells connected in series were chosen as a solar module (6 × 3 cm^2), and its V_{OC} and I_{SC} are 10.1 V and 11 mA, respectively. The solar recharging circuit includes a red LED (1.75 V). After solar charging, the coplanar LIB was able to reach 8.35 V.

■ ASSOCIATED CONTENT

Ⓢ Supporting Information

Stress formation of conventional cofacial batteries, procedure for curvy electrodes, fabrication flow for the coplanar battery, LED operation tests during bending motions, SEM images of the electrode materials, photographs and dimensional information on the knife molds, and gel electrolyte properties. This material is available free of charge via the Internet at http://pubs.acs.org.

■ AUTHOR INFORMATION

Corresponding Authors

*E-mail: (J.Y.S.) jysong@kriss.re.kr.
*E-mail: (J.W.C.) jangwookchoi@kaist.ac.kr.

Present Address

D.K.: Department of Environmental Engineering, Technical University of Denmark, Bygningstorvet, Building 115, 2800 Kgs. Lyngby, Denmark

Author Contributions

The manuscript was written through contributions of all authors. All authors have given approval to the final version of the manuscript.

Notes

The authors declare no competing financial interest.

■ ACKNOWLEDGMENTS

This work was supported by NST (National Research Council of Science & Technology, Grant 13-2-KIST) and the National Research Foundation of Korea (NRF) grant funded by the Korea government (MEST) (NRF-2012-R1A2A1A01011970 and NRF-2014R1A4A1003712).

■ REFERENCES

(1) Ahn, J.-H.; Kim, H.-S.; Lee, K. J.; Zhu, Z.; Menard, E.; Nuzzo, R. G.; Rogers, J. A. *IEEE Electron Device Lett.* **2006**, *27*, 460−462.
(2) Ju, S.; Facchetti, A.; Xuan, Y.; Liu, J.; Ishikawa, F.; Ye, P.; Zhou, C.; Marks, T. J.; Janes, D. B. *Nat. Nanotechnol.* **2007**, *2*, 378−384.
(3) Sun, Y.; Rogers, J. A. *Adv. Mater.* **2007**, *19*, 1897−1916.
(4) Baca, A. J.; Ahn, J.-H.; Sun, Y.; Meitl, M. A.; Menard, E.; Kim, H.-S.; Choi, W. M.; Kim, D.-H.; Huang, Y.; Rogers, J. A. *Angew. Chem., Int. Ed.* **2008**, *47*, 5524−5542.
(5) Sekitani, T.; Yokota, T.; Zschieschang, U.; Klauk, H.; Bauer, S.; Takeuchi, K.; Takamiya, M.; Sakurai, T.; Someya, T. *Science* **2009**, *326*, 1516−1519.
(6) Jeon, J.; Lee, H.-B.-R.; Bao, Z. *Adv. Mater.* **2013**, *25*, 850−855.
(7) Tee, B. C. K.; Chortos, A.; Dunn, R. R.; Schwartz, G.; Eason, E.; Bao, Z. *Adv. Funct. Mater.* **2014**, *24*, 5427−5434.
(8) Gustafsson, G.; Cao, Y.; Treacy, G. M.; Klavetter, F.; Colaneri, N.; Heeger, A. J. *Nature* **1992**, *357*, 477−479.
(9) Lee, S. Y.; Park, K.-I.; Huh, C.; Koo, M.; Yoo, H. G.; Kim, S.; Ah, C. S.; Sung, G. Y.; Lee, K. J. *Nano Energy* **2012**, *1*, 145−151.
(10) Jeong, C. K.; Park, K.-I.; Son, J. H.; Hwang, G.-T.; Lee, S. H.; Park, D. Y.; Lee, H. E.; Lee, H. K.; Byun, M.; Lee, K. J. *Energy Environ. Sci.* **2014**, *7*, 4035−4043.
(11) Kuang, D.; Brillet, J.; Chen, P.; Takata, M.; Uchida, S.; Miura, H.; Sumioka, K.; Zakeeruddin, S. M.; Grätzel, M. *ACS Nano* **2008**, *2*, 1113−1116.
(12) Pagliaro, M.; Ciriminna, R.; Palmisano, G. *ChemSusChem* **2008**, *1*, 880−891.
(13) Fang, X.; Yang, Z.; Qiu, L.; Sun, H.; Pan, S.; Deng, J.; Luo, Y.; Peng, H. *Adv. Mater.* **2014**, *26*, 1694−1698.
(14) Kim, S. J.; We, J. H.; Cho, B. J. *Energy Environ. Sci.* **2014**, *7*, 1959−1965.

DOI: 10.1021/nl5045814
Nano Lett. 2015, 15, 2350−2357

(15) Ahn, B. Y.; Duoss, E. B.; Motala, M. J.; Guo, X.; Park, S.-I.; Xiong, Y.; Yoon, J.; Nuzzo, R. G.; Rogers, J. A.; Lewis, J. A. *Science* **2009**, *323*, 1590−1593.
(16) Hu, L.; Kim, H. S.; Lee, J.-Y.; Peumans, P.; Cui, Y. *ACS Nano* **2010**, *4*, 2955−2963.
(17) Tobjörk, D.; Österbacka, R. *Adv. Mater.* **2011**, *23*, 1935−1961.
(18) Han, S.-T.; Zhou, Y.; Roy, V. A. L. *Adv. Mater.* **2013**, *25*, 5425−5449.
(19) Hu, L.; Choi, J. W.; Yang, Y.; Jeong, S.; La Mantia, F.; Cui, L.-F.; Cui, Y. *Proc. Natl. Acad. Sci. U.S.A.* **2009**, *106*, 21490−21494.
(20) Hu, L.; Wu, H.; La Mantia, F.; Yang, Y.; Cui, Y. *ACS Nano* **2010**, *4*, 5843−5848.
(21) Kwon, Y. H.; Woo, S.-W.; Jung, H.-R.; Yu, H. K.; Kim, K.; Oh, B. H.; Ahn, S.; Lee, S.-Y.; Song, S.-W.; Cho, J.; Shin, H.-C.; Kim, J. Y. *Adv. Mater.* **2012**, *24*, 5192−5197.
(22) Lee, Y.-H.; Kim, J.-S.; Noh, J.; Lee, I.; Kim, H. J.; Choi, S.; Seo, J.; Jeon, S.; Kim, T.-S.; Lee, J.-Y.; Choi, J. W. *Nano Lett.* **2013**, *13*, 5753−5761.
(23) Kim, J.-S.; Lee, Y.-H.; Lee, I.; Kim, T.-S.; Ryou, M.-H.; Choi, J. W. *J. Mater. Chem. A* **2014**, *2*, 10862−10868.
(24) Park, M.-H.; Noh, M.; Lee, S.; Ko, M.; Chae, S.; Sim, S.; Choi, S.; Kim, H.; Nam, H.; Park, S.; Cho, J. *Nano Lett.* **2014**, *14*, 4083−4089.
(25) Liu, S.; Wang, Z.; Yu, C.; Wu, H. B.; Wang, G.; Dong, Q.; Qiu, J.; Eychmüller, A.; Lou, X. W. *Adv. Mater.* **2013**, *25*, 3462−3467.
(26) Leijonmarck, S.; Cornell, A.; Lindbergh, G.; Wagberg, L. *J. Mater. Chem. A* **2013**, *1*, 4671−4677.
(27) Gaikwad, A. M.; Khau, B. V.; Davies, G.; Hertzberg, B.; Steingart, D. A.; Arias, A. C. *Adv. Energy Mater.* **2014**, 1401389.
(28) Wang, X.; Lu, X.; Liu, B.; Chen, D.; Tong, Y.; Shen, G. *Adv. Mater.* **2014**, *26*, 4763−4782.
(29) Gaikwad, A. M.; Steingart, D. A.; Nga Ng, T.; Schwartz, D. E.; Whiting, G. L. *Appl. Phys. Lett.* **2013**, *102*, 233302.
(30) Gaikwad, A. M.; Chu, H. N.; Qeraj, R.; Zamarayeva, A. M.; Steingart, D. A. *Energy Technol.* **2013**, *1*, 177−185.
(31) Kil, E.-H.; Choi, K.-H.; Ha, H.-J.; Xu, S.; Rogers, J. A.; Kim, M. R.; Lee, Y.-G.; Kim, K. M.; Cho, K. Y.; Lee, S.-Y. *Adv. Mater.* **2013**, *25*, 1395−1400.
(32) Russo, A.; Ahn, B. Y.; Adams, J. J.; Duoss, E. B.; Bernhard, J. T.; Lewis, J. A. *Adv. Mater.* **2011**, *23*, 3426−3430.
(33) Yang, Z.; Deng, J.; Chen, X.; Ren, J.; Peng, H. *Angew. Chem., Int. Ed.* **2013**, *52*, 13453−13457.
(34) Le, V. T.; Kim, H.; Ghosh, A.; Kim, J.; Chang, J.; Vu, Q. A.; Pham, D. T.; Lee, J.-H.; Kim, S.-W.; Lee, Y. H. *ACS Nano* **2013**, *7*, 5940−5947.
(35) Sun, H.; You, X.; Jiang, Y.; Guan, G.; Fang, X.; Deng, J.; Chen, P.; Luo, Y.; Peng, H. *Angew. Chem., Int. Ed.* **2014**, *53*, 9526−9531.
(36) Weng, W.; Sun, Q.; Zhang, Y.; Lin, H.; Ren, J.; Lu, X.; Wang, M.; Peng, H. *Nano Lett.* **2014**, *14*, 3432−3438.
(37) Li, N.; Chen, Z.; Ren, W.; Li, F.; Cheng, H.-M. *Proc. Natl. Acad. Sci. U.S.A.* **2012**, *109*, 17360−17365.
(38) Zhang, Y.; Bai, W.; Cheng, X.; Ren, J.; Weng, W.; Chen, P.; Fang, X.; Zhang, Z.; Peng, H. *Angew. Chem., Int. Ed.* **2014**, *53*, 14564−14568.
(39) Ren, J.; Li, L.; Chen, C.; Chen, X.; Cai, Z.; Qiu, L.; Wang, Y.; Zhu, X.; Peng, H. *Adv. Mater.* **2013**, *25*, 1155−1159.
(40) Lin, H.; Weng, W.; Ren, J.; Qiu, L.; Zhang, Z.; Chen, P.; Chen, X.; Deng, J.; Wang, Y.; Peng, H. *Adv. Mater.* **2014**, *26*, 1217−1222.
(41) Koo, M.; Park, K.-I.; Lee, S. H.; Suh, M.; Jeon, D. Y.; Choi, J. W.; Kang, K.; Lee, K. J. *Nano Lett.* **2012**, *12*, 4810−4816.
(42) Jung, M.-S.; Seo, J.-H.; Moon, M.-W.; Choi, J. W.; Joo, Y.-C.; Choi, I.-S. *Adv. Energy Mater.* **2015**, *5*, 1400611.
(43) Pikul, J. H.; Gang Zhang, H.; Cho, J.; Braun, P. V.; King, W. P. *Nat. Commun.* **2013**, *4*, 1732.
(44) Xu, S.; Zhang, Y.; Cho, J.; Lee, J.; Huang, X.; Jia, L.; Fan, J. A.; Su, Y.; Su, J.; Zhang, H.; Cheng, H.; Lu, B.; Yu, C.; Chuang, C.; Kim, T.-i.; Song, T.; Shigeta, K.; Kang, S.; Dagdeviren, C.; Petrov, I.; Braun, P. V.; Huang, Y.; Paik, U.; Rogers, J. A. *Nat. Commun.* **2013**, *4*, 1543.

DOI: 10.1021/nl5045814
Nano Lett. 2015, 15, 2350−2357